SUPPLEMENTAL DATA

SOX11, CD70 AND T~REG~ CELLS CONFIGURE THE TUMOR IMMUNE MICROENVIRONMENT OF AGGRESSIVE MANTLE CELL LYMPHOMA

Patricia Balsas[1,2*], Luis Veloza[3*], Guillem Clot[1,2], Marta Sureda-Gómez[1], Marta-Leonor Rodríguez[1], Christos Masaoutis[3], Gerard Frigola[3], Alba Navarro[1,2], Silvia Beà[1,2,3], Ferran Nadeu[1,2], Eva Giné[1,2,4], Armando López-Guillermo[1,2,4], Antonio Martínez[1,2,3], Inmaculada Ribera-Cortada[3], Pablo Engel[5], Leticia Quintanilla-Martinez[6], Wolfram Klapper[7], Elias Campo[1,2,3*], Virginia Amador[1,2*]

SUPPLEMENTAL METHODS

Mantle cell lymphoma cell line models

The well characterized SOX11+ MCL cell line Z138 (CRL-3001; ATCC) was used to generate the stable transduced SOX11 knockdown (Z138SOX11KD) and its control (Z138CT), using shRNA lentiviral vectors targeting specifically SOX11 and empty vector, respectively.[1] The SOX11 non-expressing MCL cell line JVM2 (ACC-12; DSMZ) was used to generate the stable transduced JVM2 cell line ectopically overexpressing SOX11 (JVM2SOX11+) and its control (JVM2CT) MCL cell line.[2] All stable transduced MCL cell lines were used for chromatin immunoprecipitation-quantitative-PCR (ChIP-qPCR). Z138CT and Z138SOX11KD were used for real time quantitative PCR (RT-qPCR) and flow cytometry (FC) experiments after CD40L, TGFβ and BCR stimulation. All the cell lines were routinely cultured at 37ºC in a humidified atmosphere with 5% CO_2 in RPMI complete medium, containing RPMI 1640 medium (Sigma-Aldrich, St Louis, MO), supplemented with 10% fetal bovine serum (FBS; Sigma), 2µM L-glutamine and 100 U/mL penicillin/streptomycin (P/S) (both from Invitrogen).

Histopathology and Immunohistochemistry studies

Immunohistochemistry (IHC) staining were performed on 2 µm thick FFPE tissues as previously[3] on an automated BenchMark ULTRA platform (Ventana, Tucson, AZ, USA), according to manufacture recommendations. The description of the antibodies used is shown in Supplemental Table S2. Tonsil sections were used as controls for all IHC staining.

Double IHC protocols with anti-human specific FOXP3 and CTLA4 antibodies (to identify effector T_{regs}) and FOXP3 and CD4 antibodies were performed sequentially in a Dako Autostainer Link 48 (Agilent, Santa Clara, CA, USA) adhering to the general manufacture guidelines, including appropriate tonsil controls. The double IHC with CD70 and Cyclin D1 antibodies were performed on an automated BenchMark ULTRA platform (Ventana). For the double IHC protocols of FOXP3 and CD4, FOXP3 was revealed with HRP Magenta chromogen (Agilent, Santa Clara, CA, USA) and CD4 with 3,3'-diaminobenzidine (horseradish peroxidase-chromogen) (Agilent, Santa Clara, CA, USA). For double IHC protocols of FOXP3 and CTLA4, FOXP3 was revealed with 3,3'-diaminobenzidine (horseradish peroxidase-chromogen) (Agilent, Santa Clara, CA, USA) and CTLA4 with HRP Magenta chromogen (Agilent, Santa Clara, CA, USA). For double IHC of CD70 and cyclin D1, CD70 was revealed with 3,3'-diaminobenzidine (horseradish peroxidase-chromogen) and cyclin D1 with Fast Red (Ventana). A case was classified as SOX11+ when more than 10% of tumor cells showed a nuclear staining pattern.[4] However, in our series all SOX11+ cases presented >50% of positive cells in the nucleus, while the SOX11- were virtually completely negative.

Consecutives sections were obtained for CD3, CD4, CD8, FOXP3, granzyme B, CD56, LAG3, CD163, CD70, CD27 and CD20 staining and FOXP3/CTLA4 double IHC staining. The evaluated intra-tumor areas were selected by overlapping with the previously marked cyclin D1 and CD3 slides. Stained sections were digitalized and five images inside the selected areas were acquired by a digital virtual microscope (Olympus BX51 microscope, Olympus, Shinjuku-ku, Tokyo, Japan) at x400 magnification (which covers a photographic area of 0.032 mm^2), as previously described[3]. For the evaluation of CD3, CD4, CD8, FOXP3, granzyme B, CD56, LAG3

and CD163 and FOXP3/CTLA4 positive immune cells, and also CD20 positive tumor cells, the number of positively stained intratumoral cells were evaluated in the five images by counting with an Olympus Cell-B™ Basic Imaging Software (Olympus) (HPF: Number of cells per high power field (x400)).

Since the ratio of the different T-cell subsets reflect the balance of effective immune response and immunosuppression, we calculated the CD4+/CD8+, FOXP3+/CD3+, FOXP3+/CD4+ and FOXP3+CTLA4+/CD4+ T-cell ratio for every case. Additionally CD20+/CD3+ cell ratio was calculated in all cases.

For CD70 IHC evaluation, the percentage of positive cells with a moderate/strong membranous staining and/or a Golgi staining pattern was calculated (around 2800-3000 cells were counted per case). The mean count of the five fields was then used.

For CD27 IHC evaluation, the tumor staining intensity was semi-quantitatively characterized as negative/weak, moderate or strong, comparing with the staining intensity of the strongly positive accompanying T cells. When the tumor cells were positive, most tumor cells maintained a relatively similar intensity. The tumor cell staining intensity and extension of tumor positive cells were integrated and quantitatively evaluated considering the mean grey value (MGV) of color deconvoluted images as a measure.[5] The stained slides were scanned with the VENTANA iScan HT slide scanner, the DAB stain was then separated by color deconvolution and converted into gray scale using the Qupath 0.2.0 software,[6] and the gray scale images were exported to ImageJ software, where the MGV of the tumoral and reactive T cell staining was measured. In order to normalize for staining intensity variation across samples due to pre-analytical factors, the tumoral/T cell MGV ratio was calculated for each slide.

NanoStringnCounter® Analysis System

The NanoStrinng Counter® Analysis System performs multiplex gene expression analysis with 730 genes from 15 different immune cell types, common checkpoint inhibitors, cancer-testis antigens and genes covering both the adaptive and innate immune response. Raw NanoString counts for each gene were subjected to technical and biological normalization using the geometric mean of 40 housekeeping genes, six positive control genes and eight negative control genes, being eliminated those genes in which geometric mean was >10-fold below the negative controls. With this panel, we obtained information about 15 immune pathways scores (13 immune cell population scores plus the gene expression of CD4 and NCAM1 (CD56)), differential expression of genes and cell type profiling (Figure 1). In this last analysis, genes previously shown to be characteristic of various cell populations are used by the software to measure their abundance (immune cell subtype scores) (nSolver 4.0, nCounter®, NanoString).

Mantle cell lymphoma gene expression profiling (GEP) dataset

Previously published GSE70910[7] GEP dataset, which contains 53 samples obtained from 41 SOX11+ MCL patients of unpurified lymph node biopsies (n=34), CD19+ purified cells isolated from concomitant lymph node tissues (n=4) and peripheral blood (n=15), was used to establish which cell compartment (tumor cells and/or non-tumoral cells from the tumor microenvironment (TME)) express the NanoString-based statistically significant downregulated or upregulated immune-related genes in SOX11+ compared to SOX11- MCL and RLN. The raw cell files of this dataset were processed using the RMA method. Two patients with peripheral

5

blood samples were considered as SOX11- MCL, based on the levels defined in our previous studies (the cutoff value used for SOX11 microarray mRNA levels was 6 expression units),[8,9] and removed from all analyses performed with this dataset. Twelve (80%) out of the 15 SOX11-positive CD19+ purified samples from peripheral blood were diagnosed as classic variant whereas the other 3 (20%) had blastoid morphology. On the other hand, 30 out of 34 (88%) unpurified lymph node samples were diagnosed as classic and 4 (12%) as blastoid/pleomorphic MCL, and 2 of the 4 cases with purified cells from the lymph nodes were blastoid/pleomorphic. The proportion of blastoid/pleomorphic cases in these subsets of samples was relatively similar to our study, 18% in the whole cohort and 27% in the subset studied with the NanoString panel (Supplemental Table S1).

Previously published and processed GSE93291[10] dataset, containing the MAS5.0 GEP of lymph node samples and survival data from 122 SOX11+ MCL patients, was used to analyze the prognostic impact of CD70 mRNA expression, the immune population score (Figure 1), the GO pathway average scores (Supplemental Table S7 and S8) and FOXP3/CD3 mRNA ratio. One case was considered as SOX11-negative MCL, based on the levels defined in our previous studies,[8,9] and removed from all analyses performed with this dataset. One outlier sample was removed from the survival analyses that included the T-cell costimulation and signaling activation pathway average score. This later sample had a score of 1.83 standard deviations below the next lowest sample and was highly influential in the cox regression analyses.

Only the probe set with the highest interquartile range for each gene was used in the analyses that included multiple genes. When genes were analyzed individually,

all probe sets of the target gene were considered and those with expression levels above background were averaged.

Chromatin Immunoprecipitation (ChIP)-quantitative-PCR (ChIP-qPCR)

We revisited our previous published Chromatin Immunoprecipitation and DNA promoter-microarray (ChIP-chip) data on MCL cell lines[1] to identify SOX11-specific binding to *CD70* regulatory region (1393-1119 pb upstream transcription start site; TSS). In vitro validation of this SOX11-specific binding was performed by ChIP-qPCR, as previously described,[1,2]

The HighCell#ChIP kit (Diagenode) along with a SOX11 specific antibody previously optimized for ChIP-chip (sc-17347; Santa Cruz Biotechnology) in SOX11+ (Z138 wild type (WT), Z138 SOX11-knockdown (Z138shSOX11KD) and its SOX11+ control (Z138CT) MCL cell lines[2]) and one SOX11- (JVM2) MCL cell lines[1]; and anti-HA antibody (Abcam) in stable transduced JVM2CT and JVM2SOX11+ MCL cell lines, generated previously in our laboratory,[2] were used for ChIP-qPCR. The ChIP experiments were carried out by following the recommendations of the kit's manufacturer. In brief, chromatin was extracted from 10×10^6 fixed MCL cell lines and lysed with Shearing Buffer S1. Chromatin was sonicated on ice with BiorupterTM sonicator from Diagenode (3 cycles of 10min [40 seconds "ON"/ 20 seconds "OFF"]). Sonicated chromatin was incubated overnight (O/N) with 2-5μg of antibodies, respectively, and then with Protein G-coated magnetic beads for 6h. After immunoprecipitation, beads were washed and DNA was decrosslinked O/N at 65ºC. DNA was eluted and purified with IPure kit (Diagenode) and quantified with Qubit ® 2.0 Fluorometer (Invitrogen Life technologies).

Specific primers for the qPCR study, to analyze enrichment of *CD70* regulatory region (Supplemental Figure S6), of the SOX11 ChIP-enriched genomic DNA regions were designed using Primers3 (http://frodo.wi.mit.edu/) (Forward primer: AACGGAGAGGGGGAGACA; Reverse primer: CTTCCACTCTCCCTGCGTCT). SOX11- and HA-ChIP DNA and 1:100 diluted input samples were analyzed in triplicate by qPCR using Fast SYBR Green Master Mix in a StepOnePlus PCR detection system (Applied Biosystems).

RNA extraction, cDNA generation and RT-qPCR

RNA extraction was performed using the RNeasy® Plus Mini Kit according to the manufacturer´s protocol instructions (Qiagen). Then, 500 ng of RNA were used to generate cDNA using the qScript™ cDNA Synthesis Kit according to the manufacturer´s protocol instructions (Quanta Bioscience). After that, cDNA was used for analyzing CD70 mRNA expression by RT-qPCR using TaqMan probes (CD70: Hs00174297_m1) and MasterMix. GUSB was used as normalization control (GUSB: Hs99999908_m1).

Flow cytometry analysis

CD70 was determined by FC using anti-CD70 (clone 113-16, Biolegend) as primary antibody and anti-mouse Pacific Blue (Invitrogen) as secondary antibody. Mouse-IgG1 (clone Sc-2025; Santa Cruz) was used as isotype control. All antibodies were incubated in PBS + 5% SFB for 1h at 4ºC and analyzed using the Attune cytometer software (Applied Biosystems)**.**

Statistical analysis

Group comparisons in the GSE70910 dataset were performed with linear mixed effects models, which took into account that several cases had multiple samples. Limma was used to identify differentially expressed genes. Genes with adjusted p value<0.15 were considered differentially expressed. P-values were adjusted for multiple testing with the Benjamini-Hochberg method (q-values). Maximally selected rank statistics was applied to find thresholds for continuous variables associated with clinical outcome (maxstat R package).

SUPPLEMENTAL TABLES

SUPPLEMENTAL TABLE S1. Clinical and pathological characteristics of primary MCL according to SOX11 expression used for NanoString GEP and CD70 IHC.

	MCL used for NanoString GEP		MCL used for IHC analysis	
	SOX11+ (N=11)	SOX11- (N=3)	SOX11+ (N=51)	SOX11- (N=13)
Median age in years (range)	63 (55-84)	59 (59-60)	61 (24-84)	60 (55-78)
Gender				
Male	10/11(91%)	1/3 (33%)	44/51 (86%)	7/11 (64%)
Female	1/11 (9%)	2/3 (67%)	7/51 (14%)	3/11 (27%)
Morphological variant				
Small cell	0/11 (0%)	3/3 (100%)	1/51 (2%)	7/13 (54%)
Classical	8/11 (73%)	0/3 (0%)	41/51 (80%)	2/13 (15%)
Blastoid/Pleomorphic	3/11 (27%)	0/3 (0%)	9/51 (18%)	4/13 (31%)
Architectural pattern				
Nodular	8/11 (73%)	2/3 (67%)	30/51 (59%)	3/12 (25%)
Diffuse	3/11 (27%)	1/3 (33%)	19/51 (37%)	812 (67%)
Mantle zone	0/11 (0%)	0/3 (0%)	2/51 (4%)	1/12 (8%)
Ki-67, median (range)	38 (10-90)	11 (5-20)	36 (2-90)	39 (3-90)
Ki-67 > 30%	6/11 (54%)	0/3 (0%)	26/51 (51%)	6/13 (46%)
17p/*TP53*/p53 alterations	2/11 (18%)	0/3 (0%)	9/43 (21%)	6/13 (46%)
17p loss	2/6 (33%)	0/0 (0%)	4/27 (15%)	4/8 (50%)
TP53 mutations	0/6 (0%)	0/2 (0%)	4/23 (17%)	3/5 (60%)
p53 positivity (IHC)	1/10 (10%)	0/3 (0%)	5/30 (17%)	4/13 (31%)
Mutated IGHV (≤ 97 identity)	0/6 (0%)	1/2 (50%)	3/28 (11%)	1/2 (50%)
Ann-Arbor Stage				
I-III	0/10 (0%)	0/2 (0%)	8/44 (18%)	1/5 (20%)
IV	10/10 (100%)	3/3 (100%)	36/44 (82%)	4/5 (80%)
Elevated LDH serum levels	6/10 (60%)	0/2 (0%)	26/44 (59%)	0/3 (0%)
Leukemic involvement	7/8 (87%)	3/3 (100%)	25/36 (69%)	4/4 (100%)
Bone marrow involvement	9/10 (90%)	3/3 (100%)	35/44 (79%)	4/5 (80%)
Splenomegaly	4/9 (44%)	2/3 (67%)	20/37 (54%)	3/4 (75%)
Survival and Treatment				
3-year OS 95% CI	66.7% [42.0-100]	100% NA	72.5% [60.3-87.1]	100%* NA
Chemotherapy at diagnosis	10/10 (100%)	0/3 (0%)	42/42 (100%)	1/4 (25%)
Relapse	4/9 (44%)	0/2 (0%)	16/38 (42%)	1/5 (20%)

MCL: mantle cell lymphoma; IHC: immunohistochemistry; IGHV: immunoglobulin heavy chain variable region; LDH: lactate dehydrogenase; OS: overall survival; CI: confidence interval. ***This data refers only to the n=4 cases with clinical data for follow-up and treatment.

SUPPLEMENTAL TABLE S2. List of antibodies used for IHC studies.

Antibody	Clone	Dilution	Source
CD20	L26	RTU	Ventana
Cyclin D1	SP4-R	RTU	Ventana
SOX11	MRQ-58	RTU	Ventana
CD5	SP19	RTU	Ventana
CD3	2GV6	RTU	Ventana
CD4	SP35	RTU	Ventana
CD8	SP57	RTU	Ventana
Granzyme B	polyclonal	RTU	Ventana
Ki-67	30-9	RTU	Ventana
p53	DO-7	RTU	Ventana
CD56	123C2	RTU	Ventana
CD163	NCL-L-CD163	1:6000	Leica
FOXP3	236A/E7	1:50	Biocare
CTLA4	F8	1:20	SantaCruz (Biotechnology)
CD70	301731	1:40	R&D systems
CD27	EPR8569	1:3000	Abcam
LAG3	17B4	1:600	Lifespan Biosciences

RTU: ready-to-use

SUPPLEMENTAL TABLE S3. 271 NanoString-based statistically significant differential expressed genes in SOX11+ vs. SOX11- nodal primary MCLs cases with adjusted P value<0.15.

Gene	logFC	adj.P.Val	Gene	logFC	adj.P.Val
HLA-DRB4	-6,562	0.008	KLRB1	-1,669	0.015
CD209	-5,002	0.000	CSF3R	-1,669	0.007
SIGLEC1	-3,794	0.000	FLT3	-1,666	0.004
MRC1	-3,461	0.000	STAT4	-1,651	0.002
LRRN3	-3,305	0.001	IL6ST	-1,632	0.002
MARCO	-3,271	0.001	TBX21	-1,608	0.005
CCL14	-2,928	0.002	HLA-G	-1,6	0.009
CXCL12	-2,86	0.002	ITGA1	-1,597	0.002
CD163	-2,731	0.004	FCGR2A	-1,591	0.012
CD36	-2,618	0.003	CD33	-1,587	0.002
F13A1	-2,511	0.011	CD96	-1,586	0.024
COLEC12	-2,423	0.002	THBS1	-1,578	0.014
TNFSF11	-2,416	0.000	TXNIP	-1,57	0.002
TNFRSF11A	-2,402	0.003	IDO1	-1,56	0.005
CD160	-2,395	0.002	IFITM1	-1,557	0.023
CMA1	-2,23	0.010	CXCR3	-1,545	0.005
CTSL	-2,152	0.001	CCR9	-1,539	0.032
KLRD1	-2,152	0.003	CD28	-1,538	0.012
CCL21	-2,137	0.015	CD3G	-1,535	0.017
CD40LG	-2,134	0.007	IL23R	-1,529	0.019
TPSAB1	-2,12	0.088	MAF	-1,527	0.010
ITGA6	-2,105	0.003	PDGFRB	-1,526	0.003
CD1B	-2,087	0.012	TLR3	-1,522	0.001
IL7R	-2,05	0.012	TXK	-1,511	0.010
BTLA	-2,037	0.006	CFI	-1,51	0.003
CTSG	-2,016	0.035	CLEC7A	-1,51	0.004
FCER1A	-2,01	0.004	NT5E	-1,5	0.030
S100A8	-2	0.018	AXL	-1,48	0.034
CCL18	-1,985	0.088	MS4A2	-1,461	0.015
CFD	-1,98	0.016	IL1A	-1,43	0.045
XCL2	-1,976	0.018	SERPING1	-1,425	0.005
PPARG	-1,912	0.001	HLA-DPB1	-1,424	0.024
C1QB	-1,907	0.045	AIRE	-1,419	0.080
SELL	-1,902	0.025	CD244	-1,414	0.006
CXCL5	-1,896	0.085	CCL16	-1,403	0.011
ANXA1	-1,883	0.001	C1S	-1,401	0.009
KLRF1	-1,86	0.028	ITGA5	-1,398	0.006
CD86	-1,842	0.002	CR1	-1,383	0.073
FCGR3A	-1,821	0.033	SPP1	-1,376	0.133
PDGFC	-1,816	0.001	CASP1	-1,374	0.004
LAMP3	-1,812	0.041	PTPRC	-1,372	0.041

IL1R1	-1,809	0.007	**AMICA1**	-1,357	0.010
DPP4	-1,766	0.001	**S100B**	-1,351	0.123
NRP1	-1,74	0.004	**NOS2A**	-1,35	0.015
GNLY	-1,727	0.029	**TLR8**	-1,34	0.022
SH2D1B	-1,7	0.004	**IL6R**	-1,325	0.024
CD3D	-1,687	0.009	**PDCD1LG2**	-1,306	0.005
CD4	-1,687	0.003	**CDH5**	-1,302	0.004
HLA-DPA1	-1,282	0.005	**ITGB3**	-0,949	0.087
RORC	-1,273	0.008	**BMI1**	-0,949	0.015
IL15	-1,263	0.017	**SH2D1A**	-0,944	0.101
SLAMF1	-1,257	0.045	**CTSS**	-0,944	0.012
C2	-1,249	0.074	**LRP1**	-0,942	0.088
CD34	-1,233	0.023	**REPS1**	-0,942	0.030
LGALS3	-1,215	0.025	**S100A12**	-0,941	0.057
CD1E	-1,213	0.080	**CFP**	-0,94	0.080
VCAM1	-1,198	0.029	**STAT5B**	-0,93	0.030
PTGDR2	-1,197	0.021	**FLT3LG**	-0,929	0.033
C7	-1,195	0.032	**CCL23**	-0,926	0.030
NCAM1	-1,189	0.048	**CEBPB**	-0,922	0.012
C1QA	-1,179	0.111	**FCER1G**	-0,92	0.133
VEGFC	-1,164	0.010	**CD59**	-0,918	0.051
IFNGR1	-1,156	0.009	**CTAG1B**	-0,916	0.030
SSX1	-1,15	0.013	**ITK**	-0,909	0.095
TNFRSF1A	-1,149	0.004	**CD48**	-0,907	0.018
KLRG1	-1,148	0.084	**SPANXB1**	-0,903	0.082
ABCB1	-1,141	0.133	**CD164**	-0,901	0.030
CSF1	-1,14	0.025	**IL18RAP**	-0,901	0.095
IL3RA	-1,133	0.066	**CFB**	-0,899	0.032
C3	-1,128	0.095	**ICOS**	-0,893	0.096
CD247	-1,127	0.030	**TNFSF18**	-0,884	0.111
DOCK9	-1,12	0.015	**IL12B**	-0,879	0.032
MNX1	-1,117	0.101	**ITGB2**	-0,875	0.065
CXCL16	-1,107	0.020	**VEGFA**	-0,873	0.032
A2M	-1,106	0.028	**TLR5**	-0,871	0.033
SELPLG	-1,1	0.014	**TARP**	-0,866	0.149
CCL13	-1,093	0.148	**PRM1**	-0,865	0.067
F2RL1	-1,09	0.030	**TAL1**	-0,856	0.103
IL2RG	-1,089	0.010	**CXCL10**	-0,846	0.102
CCR4	-1,086	0.029	**CREB5**	-0,846	0.084
ENG	-1,082	0.033	**TNFRSF10C**	-0,819	0.110
C3AR1	-1,079	0.010	**CCR2**	-0,816	0.113
TNFSF10	-1,077	0.017	**LTBR**	-0,813	0.030
IL2	-1,074	0.064	**CX3CR1**	-0,81	0.084
HLA-DRA	-1,066	0.015	**ATG5**	-0,808	0.030
C1R	-1,065	0.018	**CTSH**	-0,8	0.080
ITGB1	-1,065	0.024	**GATA3**	-0,796	0.113
COL3A1	-1,061	0.015	**IL12RB2**	-0,794	0.117
TCF7	-1,044	0.094	**TNFSF13B**	-0,794	0.050

THBD	-1,037	0.046	**TANK**	-0,788	0.033
RORA	-1,034	0.032	**CMKLR1**	-0,779	0.067
ITGA2	-1,031	0.022	**CD46**	-0,772	0.033
IL32	-1,03	0.039	**JAK1**	-0,763	0.084
PECAM1	-1,001	0.010	**MAPK1**	-0,754	0.088
IL34	-1	0.024	**PSEN2**	-0,753	0.056
CXCL14	-0,985	0.108	**BST1**	-0,74	0.074
CD3E	-0,963	0.057	**CX3CL1**	-0,736	0.084
NFKB1	-0,73	0.080	**CXCR5**	0,823	0.086
MR1	-0,695	0.111	**TLR9**	0,845	0.100
JAK2	-0,691	0.061	**CD79A**	0,852	0.023
CASP10	-0,681	0.096	**SPN**	0,862	0.088
CDH1	-0,66	0.117	**EGR2**	0,886	0.116
HLA-E	-0,658	0.042	**HLA-DRB3**	0,895	0.088
MAGEA4	-0,652	0.102	**IRF5**	0,931	0.057
NFATC3	-0,644	0.099	**CEACAM1**	0,954	0.086
TNFRSF8	-0,644	0.133	**MIF**	0,975	0.061
IRF8	-0,642	0.113	**TFEB**	0,989	0.011
TNFRSF1B	-0,632	0.129	**CD19**	1,008	0.047
FAS	-0,63	0.120	**PAX5**	1,063	0.007
IRF2	-0,622	0.038	**IRF4**	1,095	0.033
IL15RA	-0,619	0.119	**CD37**	1,107	0.014
ICAM2	-0,615	0.133	**LTK**	1,124	0.129
ETS1	-0,611	0.088	**ICOSLG**	1,131	0.030
F12	-0,611	0.096	**ADORA2A**	1,141	0.011
IRGM	-0,598	0.096	**CD70**	1,152	0.144
ATF1	-0,563	0.062	**BCL2**	1,161	0.033
RPS6	-0,558	0.084	**ENTPD1**	1,206	0.133
CYLD	-0,558	0.095	**CCL3**	1,237	0.037
ICAM3	-0,557	0.094	**TNFSF13**	1,254	0.086
PSEN1	-0,556	0.114	**PRKCE**	1,272	0.014
FCGR1A	-0,508	0.113	**CD24**	1,281	0.052
NFKBIA	-0,505	0.113	**SH2B2**	1,321	0.022
ATF2	-0,501	0.080	**CD38**	1,337	0.085
MAPK14	-0,424	0.123	**CXCL9**	1,338	0.112
ILF3	0,436	0.102	**CDK1**	1,399	0.066
GTF3C1	0,494	0.092	**SYT17**	1,41	0.015
STAT6	0,531	0.085	**CD3EAP**	1,437	0.010
BAX	0,538	0.120	**TNFRSF18**	1,482	0.017
PIN1	0,549	0.062	**CD79B**	1,796	0.007
TIRAP	0,558	0.100	**BIRC5**	1,908	0.029
MAPKAPK2	0,56	0.095	**TTK**	2,133	0.006
MYD88	0,627	0.061	**MSR1**	2,176	0.119
TNFRSF13C	0,672	0.135	**PBK**	2,274	0.010
IRF3	0,759	0.098	**USP9Y**	2,703	0.070
FADD	0,778	0.080	**IL17RB**	3,067	0.022
TNFRSF9	0,797				

FC: Fold Change; adj.P.Val: adjusted p-value

Supplemental Table S4. 395 NanoString-based statistically significant differential expressed genes in SOX11+ nodal MCLs vs. RLN primary cases with adjusted P value<0.15 .

Gene	logFC	adj.P.Val	Gene	logFC	adj.P.Val
CCL18	-4,344	0.000	FLT3	-1,994	0.000
TREM1	-3,415	0.003	C3	-1,977	0.001
AICDA	-3,282	0.000	IL4R	-1,966	0.000
GZMB	-3,092	0.000	ITGA6	-1,962	0.001
LRRN3	-3,049	0.000	C1QB	-1,955	0.003
MRC1	-2,901	0.000	ABCB1	-1,914	0.001
F13A1	-2,824	0.000	ICOS	-1,905	0.000
CD209	-2,811	0.001	CTLA4	-1,901	0.000
IL21	-2,76	0.000	CLEC7A	-1,893	0.000
CLEC4C	-2,726	0.002	AIRE	-1,876	0.001
CCL17	-2,716	0.000	CD200	-1,871	0.000
CCL24	-2,707	0.003	IL6R	-1,868	0.000
CCL13	-2,707	0.000	CCL23	-1,858	0.000
CD1B	-2,649	0.000	CD3D	-1,849	0.000
FCER1A	-2,649	0.000	CXCR2	-1,833	0.004
LAMP3	-2,645	0.000	AMICA1	-1,83	0.000
S100A8	-2,587	0.031	ITGA5	-1,827	0.000
LIF	-2,538	0.000	CD247	-1,815	0.000
SLAMF1	-2,511	0.000	C7	-1,803	0.000
S100B	-2,497	0.000	SERPINB2	-1,803	0.049
KLRB1	-2,452	0.000	COL3A1	-1,795	0.000
CCL21	-2,44	0.000	KLRD1	-1,792	0.000
CD40LG	-2,43	0.000	TPSAB1	-1,791	0.049
CCL14	-2,336	0.000	SELL	-1,788	0.002
FCER2	-2,314	0.011	MAF	-1,782	0.000
GNLY	-2,238	0.001	TLR8	-1,778	0.000
NRP1	-2,229	0.000	SH2D1B	-1,776	0.000
CXCL12	-2,224	0.000	CCL26	-1,775	0.006
ANXA1	-2,182	0.003	CD3E	-1,751	0.000
SIGLEC1	-2,163	0.000	S100A12	-1,727	0.009
CCL19	-2,16	0.000	RORC	-1,723	0.000
THBD	-2,152	0.000	FCGR3A	-1,715	0.003
BTLA	-2,147	0.000	MME	-1,706	0.043
IL23R	-2,121	0.001	CD1E	-1,705	0.001
IL1R1	-2,109	0.000	MS4A2	-1,701	0.002
DPP4	-2,084	0.000	ITK	-1,691	0.000
CD28	-2,08	0.000	LCN2	-1,689	0.101
CD36	-2,053	0.000	KLRC2	-1,673	0.072
TNFRSF11A	-2,051	0.000	ITGB3	-1,635	0.001
NT5E	-2,05	0.000	TNFRSF8	-1,633	0.000
SPINK5	-2,048	0.072	CD3G	-1,63	0.000

CD163	-2,047	0.003	**LTBR**	-1,629	0.000
IL7R	-2,028	0.002	**CD59**	-1,625	0.000
IL1R2	-2,01	0.002	**IDO1**	-1,618	0.000
CCR2	-2,004	0.000	**CD86**	-1,615	0.000
CFI	-1,608	0.000	**IL34**	-1,392	0.000
ITGA2	-1,604	0.001	**PPARG**	-1,374	0.000
IFITM1	-1,599	0.001	**CDH5**	-1,373	0.000
ITGA1	-1,596	0.001	**NCAM1**	-1,372	0.002
SERPING1	-1,596	0.000	**IL1A**	-1,37	0.016
TXK	-1,592	0.001	**C1R**	-1,355	0.001
THBS1	-1,59	0.005	**SELPLG**	-1,349	0.000
PDGFRB	-1,579	0.000	**TNFRSF1A**	-1,343	0.000
IL1RN	-1,577	0.132	**SPP1**	-1,341	0.021
TCF7	-1,573	0.001	**IL2RB**	-1,331	0.003
A2M	-1,57	0.000	**CTSG**	-1,327	0.045
CCL8	-1,567	0.000	**BCL6**	-1,317	0.002
FOS	-1,558	0.061	**LGALS3**	-1,305	0.003
CD7	-1,558	0.003	**TLR5**	-1,303	0.000
TAL1	-1,55	0.001	**CFB**	-1,299	0.001
TNFSF13B	-1,547	0.000	**TNFSF10**	-1,288	0.000
PTGDR2	-1,545	0.000	**IL12RB2**	-1,287	0.001
MUC1	-1,543	0.006	**IL18R1**	-1,271	0.005
IL6ST	-1,54	0.000	**CDH1**	-1,263	0.001
KLRF1	-1,535	0.004	**TNFRSF17**	-1,258	0.058
CCL20	-1,533	0.100	**MEFV**	-1,254	0.001
IL3RA	-1,523	0.001	**KIT**	-1,246	0.031
KLRC1	-1,521	0.073	**ENG**	-1,245	0.001
STAT4	-1,514	0.000	**CD34**	-1,231	0.003
C1QA	-1,509	0.004	**CD14**	-1,231	0.004
CD96	-1,508	0.003	**LILRB3**	-1,231	0.005
F12	-1,504	0.000	**C1S**	-1,23	0.003
FCGR2A	-1,494	0.000	**TARP**	-1,224	0.004
F2RL1	-1,482	0.001	**CCL2**	-1,216	0.002
AXL	-1,481	0.002	**SOCS1**	-1,215	0.003
IL18RAP	-1,476	0.001	**CXCL14**	-1,203	0.008
CD2	-1,459	0.001	**GZMM**	-1,197	0.008
CREB5	-1,456	0.000	**ITGB1**	-1,196	0.000
FUT7	-1,451	0.005	**CD160**	-1,193	0.009
CD4	-1,448	0.000	**CD1A**	-1,191	0.031
GATA3	-1,442	0.000	**XCL2**	-1,182	0.047
IL2	-1,438	0.001	**CCL16**	-1,181	0.003
CEACAM6	-1,434	0.053	**RORA**	-1,179	0.010
PDGFC	-1,43	0.001	**CLEC4A**	-1,179	0.002
IL1RL1	-1,424	0.001	**CCL11**	-1,177	0.025
ADA	-1,424	0.000	**IL1B**	-1,169	0.041
CFD	-1,423	0.006	**CCR1**	-1,167	0.031
PTPRC	-1,422	0.002	**LRP1**	-1,16	0.006
DOCK9	-1,412	0.000	**CCR4**	-1,159	0.004

HLA-DPB1	-1,403	0.007	**IFI27**	-1,148	0.010
MEF2C	-1,398	0.009	**IL17A**	-1,147	0.099
CMA1	-1,396	0.020	**SLAMF7**	-1,146	0.014
CCR9	-1,143	0.011	**EGR1**	-0,919	0.074
CXCL16	-1,137	0.001	**C2**	-0,914	0.036
SH2D1A	-1,135	0.007	**NCR1**	-0,912	0.006
CCND3	-1,135	0.001	**IL6**	-0,91	0.105
FCER1G	-1,128	0.011	**SSX1**	-0,909	0.013
FLT3LG	-1,123	0.005	**MAGEA1**	-0,904	0.011
IL15	-1,122	0.003	**C3AR1**	-0,891	0.001
IL1RL2	-1,103	0.003	**TXNIP**	-0,888	0.002
CD207	-1,099	0.004	**FN1**	-0,887	0.040
LILRA5	-1,097	0.004	**PDCD1**	-0,885	0.065
CSF2RB	-1,094	0.005	**IL4**	-0,881	0.061
TREM2	-1,083	0.014	**CD33**	-0,863	0.004
ZAP70	-1,081	0.024	**DUSP4**	-0,858	0.110
MCAM	-1,071	0.003	**SSX4**	-0,852	0.016
CEBPB	-1,064	0.001	**DUSP6**	-0,85	0.008
STAT5B	-1,05	0.001	**C4B**	-0,849	0.113
ITGB4	-1,044	0.026	**CLU**	-0,849	0.037
PRM1	-1,035	0.005	**MPPED1**	-0,844	0.080
PVR	-1,03	0.000	**CCR3**	-0,843	0.055
TBX21	-1,026	0.003	**CSF2**	-0,841	0.018
LBP	-1,016	0.016	**CSF3R**	-0,836	0.019
TNFSF11	-1,016	0.019	**TICAM2**	-0,833	0.011
C6	-1,014	0.012	**HLA-DPA1**	-0,826	0.062
RAG1	-1,009	0.006	**C1QBP**	-0,824	0.008
LILRA1	-1,008	0.004	**IL17F**	-0,822	0.039
CXCR3	-1,002	0.002	**MASP1**	-0,811	0.009
LAG3	-1	0.068	**PDCD1LG2**	-0,81	0.017
C4BPA	-0,996	0.005	**TNFRSF1B**	-0,8	0.008
CD8B	-0,995	0.031	**FOXP3**	-0,799	0.047
RRAD	-0,995	0.016	**LAIR2**	-0,791	0.029
IL32	-0,99	0.003	**THY1**	-0,791	0.027
TLR3	-0,99	0.003	**IL21R**	-0,791	0.051
FCGR1A	-0,986	0.003	**CARD9**	-0,788	0.041
CCL1	-0,981	0.017	**STAT3**	-0,777	0.003
IFNGR1	-0,981	0.001	**IL13RA2**	-0,777	0.049
ICAM4	-0,974	0.021	**ULBP2**	-0,775	0.036
CX3CR1	-0,973	0.003	**TNFSF18**	-0,769	0.033
VEGFC	-0,972	0.006	**CMKLR1**	-0,753	0.009
CD48	-0,97	0.001	**CDKN1A**	-0,745	0.031
CD244	-0,96	0.006	**IL1RAPL2**	-0,739	0.011
ZNF205	-0,95	0.016	**IFNB1**	-0,739	0.080
CTSL	-0,937	0.016	**PECAM1**	-0,736	0.020
CD164	-0,935	0.004	**KIR_Inhibiting_ Subgroup_2**	-0,729	0.075
IL12B	-0,929	0.004	**REPS1**	-0,726	0.025

			KIR_Inhibiting_Subgroup_1	-0,717	0.050
CXCL10	-0,925	0.057			
SLC11A1	-0,921	0.027	XCR1	-0,717	0.064
TNFSF14	-0,92	0.001	VEGFA	-0,71	0.039
CASP10	-0,708	0.034	CCL15	-0,508	0.131
IFNA7	-0,697	0.022	IL25	-0,502	0.057
ISG20	-0,693	0.089	LY96	-0,501	0.089
ANP32B	-0,684	0.050	CRP	-0,491	0.079
SLAMF6	-0,669	0.048	NFATC3	-0,489	0.079
CEACAM8	-0,666	0.054	CD81	-0,485	0.041
EGR2	-0,666	0.068	ATG5	-0,484	0.068
PTGS2	-0,662	0.145	BST1	-0,482	0.143
TNFSF12	-0,661	0.011	HLA-E	-0,468	0.042
CYLD	-0,661	0.007	TANK	-0,457	0.065
ARG1	-0,658	0.101	IL2RG	-0,453	0.103
TNFRSF10C	-0,658	0.042	ICAM1	-0,412	0.100
IL15RA	-0,655	0.019	PSMD7	-0,392	0.099
CSF3	-0,654	0.087	MAPK14	-0,382	0.056
OSM	-0,653	0.106	TFE3	-0,369	0.115
IL24	-0,646	0.115	ATG16L1	-0,314	0.123
IL11	-0,645	0.089	MYD88	0,379	0.144
CD63	-0,644	0.034	INPP5D	0,4	0.104
MAP2K1	-0,644	0.012	ILF3	0,407	0.040
CSF1	-0,643	0.041	REL	0,434	0.089
CD276	-0,64	0.058	ABL1	0,487	0.099
ITGB2	-0,637	0.057	TNFRSF9	0,519	0.130
ITGAL	-0,635	0.101	IL10RA	0,521	0.107
IL26	-0,629	0.053	TLR4	0,542	0.062
MERTK	-0,628	0.087	STAT6	0,584	0.026
CXCR1	-0,624	0.143	CYFIP2	0,606	0.029
FYN	-0,619	0.049	IL7	0,612	0.128
CASP1	-0,605	0.025	ST6GAL1	0,638	0.026
VCAM1	-0,604	0.033	SMAD3	0,654	0.025
ATM	-0,602	0.089	MAP3K1	0,705	0.008
CTAG1B	-0,6	0.074	CARD11	0,733	0.015
TNFSF8	-0,598	0.103	SYK	0,751	0.017
SPA17	-0,585	0.031	POU2F2	0,78	0.038
ETS1	-0,581	0.049	SH2B2	0,786	0.085
CCL27	-0,579	0.075	TLR6	0,806	0.004
TIGIT	-0,578	0.137	LYN	0,81	0.005
IRF8	-0,576	0.057	ENTPD1	0,839	0.089
SBNO2	-0,575	0.028	SYT17	0,878	0.023
SIGIRR	-0,573	0.130	CCL4	0,904	0.082
CD68	-0,571	0.106	PRKCE	0,926	0.007
TNFRSF14	-0,569	0.012	PAX5	0,963	0.021
RPS6	-0,566	0.018	BTK	1,007	0.008
SPANXB1	-0,565	0.144	BLNK	1,01	0.001
CTAGE1	-0,541	0.139	TFEB	1,013	0.001

FPR2	-0,514	0.101	**TNFSF4**	1,046	0.068
IFNL2	-0,513	0.146	**CD1C**	1,067	0.141
PSEN2	-0,509	0.057	**CD19**	1,075	0.016
KLRK1	1,11	0.090	**IRF5**	1,48	0.000
CXCR5	1,165	0.003	**TNFRSF13C**	1,526	0.000
TLR10	1,181	0.001	**IRAK2**	1,531	0.001
CD79A	1,185	0.005	**BLK**	1,56	0.000
CD37	1,198	0.004	**CAMP**	1,585	0.036
FCGR2B	1,209	0.003	**CEACAM1**	1,59	0.001
BCL2	1,262	0.006	**CD1D**	1,741	0.002
MS4A1	1,302	0.001	**CD24**	1,841	0.001
TLR9	1,423	0.003	**MSR1**	1,861	0.047
CD79B	1,425	0.008	**TNFRSF13B**	2,058	0.001
LILRA4	1,431	0.103	**CD70**	2,289	0.000
			IL17RB	3,132	0.000

FC: Fold Change; adj.P.Val: adjusted p-value

SUPPLEMENTAL TABLE S5. 12 NanoString-based statistically significant differential expressed genes in SOX11- vs. RLN primary cases with adjusted P value<0.15 .

Gene	logFC	adj.P.Val
TNRFSF13B	-2.054	0.111
IL7	-1.279	0.145
BLK	-1.204	0.149
CCR2	1.187	0.111
CD200	1.497	0.121
BCL6	1.703	0.080
CCL19	1.803	0.020
GZMB	1.977	0.130
IL4R	2.035	0.111
LIF	2.098	0.040
CCL17	2.370	0.145
PBK	2.595	0.149

FC: Fold Change; adj.P.Val: adjusted p-value

SUPPLEMENTAL TABLE S6. Differential expression of the 190 genes, significantly downregulated in SOX11+ compared to SOX11- nodal MCLs and RLNs, in unpurified nodal samples (unpurified LN; n=34) compared to CD19+ purified lymph nodes (CD19+ LN; n=4) and CD19+ purified peripheral blood samples (CD19+ PB; n=15) of pretreated SOX11+ MCL cases (GSE70910).

	Unpurified LN vs CD19+ purified PB		Unpurified LN vs CD19+ purified LN	
	log2(FC)	adj.P.val	log2(FC)	adj.P.val
CXCL14	6,569	0,000	6,381	0,000
VCAM1	7,192	0,000	6,175	0,000
CCL21	6,014	0,000	6,141	0,000
COL3A1	5,314	0,000	5,304	0,000
A2M	4,617	0,000	4,654	0,000
C1S	5,032	0,000	4,560	0,000
CXCL12	6,100	0,000	4,183	0,000
C3	4,341	0,000	4,170	0,000
CXCL10	4,524	0,000	4,152	0,000
IL6ST	3,931	0,000	4,031	0,000
CDH1	4,157	0,000	4,003	0,000
C7	4,091	0,000	3,897	0,000
PDGFC	3,646	0,000	3,831	0,000
MAF	3,998	0,000	3,829	0,000
SERPING1	3,479	0,000	3,694	0,000
IL7R	3,849	0,000	3,611	0,000
IL32	4,283	0,000	3,575	0,000
C1QA	4,010	0,000	3,532	0,000
C1QB	3,412	0,000	3,480	0,000
ANXA1	2,977	0,000	3,154	0,000
TNFSF11	3,618	0,000	3,109	0,000
THBD	2,810	0,000	3,096	0,000
C1R	3,563	0,000	3,080	0,000
IL1R1	3,194	0,000	2,899	0,000
THBS1	3,084	0,000	2,748	0,001
TNFSF13B	2,550	0,000	2,715	0,000
FCER1G	2,299	0,000	2,704	0,000
CD3D	3,212	0,000	2,689	0,000
ITK	3,439	0,000	2,665	0,000
CD28	2,770	0,000	2,624	0,000
CTSL	2,496	0,000	2,609	0,000
LGALS3	3,250	0,000	2,589	0,000
S100A8	-0,556	0,353	2,558	0,024
SH2D1A	3,261	0,000	2,444	0,000
LAMP3	2,356	0,000	2,439	0,000

CMKLR1	1,870	0,000	2,289	0,000
RORA	2,170	0,000	2,172	0,004
CX3CR1	0,778	0,012	2,136	0,001
CCL18	2,194	0,000	2,108	0,009
IL2RG	0,532	0,264	2,095	0,022
CD4	2,028	0,000	2,075	0,002
VEGFC	1,790	0,000	2,041	0,000
C3AR1	1,293	0,000	2,037	0,000
TARP	2,372	0,000	2,035	0,002
IDO1	1,987	0,000	1,980	0,000
CDH5	2,003	0,000	1,967	0,001
CLEC7A	1,863	0,000	1,931	0,003
CFD	1,547	0,002	1,892	0,011
CD3E	2,155	0,000	1,891	0,003
STAT4	1,793	0,000	1,845	0,000
IL15	1,408	0,001	1,828	0,002
CD3G	2,099	0,000	1,783	0,001
XCL2	2,897	0,000	1,758	0,008
TLR8	1,253	0,001	1,753	0,001
ITGA6	2,061	0,000	1,752	0,000
CD247	2,071	0,000	1,728	0,001
MRC1	1,392	0,001	1,721	0,003
IL6R	1,675	0,000	1,667	0,004
KLRB1	2,061	0,000	1,651	0,003
TNFRSF1A	2,215	0,000	1,649	0,001
CCL14	1,842	0,000	1,634	0,004
AXL	1,461	0,000	1,629	0,002
ITGB2	1,855	0,000	1,581	0,003
CD36	1,642	0,001	1,527	0,029
CFB	1,660	0,000	1,525	0,000
NRP1	1,783	0,000	1,507	0,006
TPSAB1	1,560	0,001	1,480	0,021
C2	1,213	0,000	1,470	0,002
TLR5	1,220	0,000	1,372	0,000
CD163	1,271	0,004	1,341	0,040
JAML	0,714	0,010	1,291	0,005
ICOS	1,597	0,000	1,251	0,001
CD164	0,788	0,056	1,228	0,076
TNFRSF1B	1,065	0,001	1,217	0,009
ENG	1,390	0,000	1,181	0,001
CXCL16	0,409	0,020	1,110	0,001
TNFSF10	0,778	0,001	1,079	0,002
CD96	1,091	0,005	1,076	0,049
PDGFRB	1,283	0,000	1,031	0,004
IFNGR1	1,422	0,000	1,021	0,001
CD1E	1,121	0,003	1,021	0,058
CFI	1,315	0,000	0,965	0,004
CD59	1,982	0,000	0,926	0,034

SIGLEC1	0,868	0,002	0,920	0,011
IFITM1	1,938	0,000	0,915	0,017
CD86	1,190	0,001	0,914	0,031
SELPLG	0,570	0,002	0,894	0,002
IL1A	0,716	0,004	0,887	0,022
IL15RA	0,896	0,000	0,871	0,003
NT5E	0,677	0,000	0,841	0,001
CXCR3	1,237	0,000	0,835	0,008
SLAMF1	1,471	0,000	0,829	0,008
VEGFA	2,919	0,000	0,801	0,120
IL3RA	0,960	0,000	0,793	0,003
ITGB1	1,342	0,002	0,793	0,124
CD34	0,891	0,001	0,778	0,023
FLT3LG	-0,367	0,168	0,773	0,096
PDCD1LG2	0,527	0,002	0,772	0,004
CD244	0,501	0,003	0,757	0,005
TXK	0,849	0,000	0,724	0,012
TXNIP	-0,842	0,002	0,718	0,028
SELL	0,683	0,082	0,691	0,264
DOCK9	0,506	0,020	0,676	0,030
PECAM1	0,664	0,007	0,660	0,045
SPP1	0,768	0,002	0,647	0,032
ITGA5	0,629	0,001	0,616	0,010
S100B	0,682	0,002	0,605	0,041
GNLY	0,433	0,128	0,593	0,213
CD33	0,428	0,002	0,563	0,010
CSF3R	0,233	0,016	0,554	0,002
STAT5B	0,108	0,596	0,548	0,122
LRRN3	0,580	0,019	0,543	0,109
LTBR	0,447	0,004	0,534	0,022
CD160	0,574	0,008	0,530	0,074
GATA3	2,067	0,000	0,525	0,390
DPP4	0,612	0,001	0,493	0,038
IL12RB2	0,457	0,007	0,489	0,059
BST1	0,458	0,002	0,457	0,031
CEBPB	0,245	0,049	0,447	0,027
CD209	0,540	0,021	0,446	0,162
NCAM1	0,256	0,017	0,441	0,013
HLA-E	-0,127	0,408	0,439	0,090
CTSG	0,376	0,028	0,436	0,088
CSF1	0,762	0,000	0,435	0,047
CASP1	0,366	0,109	0,435	0,204
F2RL1	0,523	0,001	0,434	0,030
FLT3	0,375	0,006	0,390	0,045
CMA1	0,254	0,024	0,376	0,026
TCF7	0,148	0,497	0,347	0,312
NFATC3	0,096	0,791	0,346	0,583
TNFRSF11A	0,238	0,008	0,291	0,022

ITGA1	0,341	0,002	0,286	0,036
HLA-DPB1	-0,547	0,027	0,284	0,448
PPARG	0,132	0,307	0,283	0,204
HLA-DPA1	-1,257	0,003	0,280	0,608
KLRD1	0,288	0,026	0,278	0,107
IL18RAP	0,478	0,004	0,271	0,204
ITGA2	0,371	0,000	0,270	0,008
CCL13	0,270	0,006	0,267	0,056
ETS1	-0,427	0,144	0,244	0,615
F13A1	1,526	0,003	0,238	0,722
FCGR3A	0,080	0,517	0,237	0,264
CD40LG	0,334	0,011	0,236	0,222
CCR2	0,903	0,007	0,197	0,671
PSEN2	-0,197	0,137	0,195	0,350
CCL16	-0,115	0,182	0,193	0,189
TBX21	0,022	0,913	0,170	0,604
TLR3	0,209	0,003	0,155	0,063
IL12B	0,173	0,011	0,147	0,079
ABCB1	-0,464	0,119	0,139	0,755
FCER1A	0,116	0,111	0,116	0,284
CCR4	0,125	0,167	0,104	0,491
AIRE	-0,111	0,258	0,094	0,577
PTPRC	0,038	0,895	0,081	0,858
LRP1	0,003	0,972	0,079	0,639
S100A12	-0,872	0,020	0,057	0,916
CCL23	0,047	0,267	0,046	0,461
TANK	0,028	0,913	0,031	0,930
PRM1	-0,138	0,092	0,022	0,873
CD1B	0,041	0,639	0,007	0,959
SSX1	-0,042	0,445	-0,015	0,873
KLRF1	-0,202	0,419	-0,039	0,913
CREB5	-0,025	0,737	-0,043	0,737
TNFRSF8	-0,030	0,692	-0,046	0,722
IL34	-0,169	0,116	-0,048	0,784
RORC	-0,113	0,213	-0,052	0,737
SH2D1B	-0,118	0,180	-0,068	0,628
TNFRSF10C	-0,043	0,542	-0,069	0,572
TNFSF18	-0,171	0,028	-0,099	0,399
FCGR1A	-0,065	0,041	-0,112	0,020
CTAG1B	-0,262	0,004	-0,113	0,362
PTGDR2	-0,296	0,005	-0,119	0,411
ITGB3	-0,064	0,353	-0,125	0,291
MS4A2	-0,031	0,652	-0,133	0,260
RPS6	-0,146	0,035	-0,151	0,169
IL2	-0,036	0,614	-0,155	0,175
CCR9	-0,322	0,034	-0,171	0,418
MAPK14	0,135	0,440	-0,201	0,496
FCGR2A	-0,870	0,000	-0,207	0,327

CASP10	0,270	0,102	-0,222	0,353
IRF8	-0,769	0,000	-0,236	0,142
IL23R	-0,115	0,065	-0,242	0,026
ATG5	0,017	0,913	-0,277	0,234
TAL1	-0,268	0,060	-0,301	0,196
F12	-0,366	0,003	-0,302	0,069
SPANXB1	-0,195	0,007	-0,310	0,010
BTLA	-1,078	0,005	-0,364	0,477
CD48	-0,051	0,745	-0,414	0,103
REPS1	-0,446	0,045	-0,512	0,130
CYLD	-0,615	0,001	-0,608	0,023

FC: Fold Change; adj.P.Val: adjusted p-value

SUPPLEMENTAL TABLE S7. DAVID gene ontology functional annotations of the 124 NanoString-based downregulated genes in SOX11+ vs. SOX11- nodal MCLs and RLN primary cases, statistically significant upregulated in unpurified LN samples compare to purified LN and PB samples from MCL patients, and their association with OS of 122 SOX11+ MCL patients (GSE93291).

Functional annotation cluster	Enrichment score	Genes	adj. P. Val	COX reg. P. Val
Cytokine-cytokine receptor interaction	8.2	*IL1R1, IL6ST, CSF1, CXCR3, IL15, IL7R, CXCL12, CXCL10, IL12RB2, TNFRSF1A, TNFRSF1B, TNFRSF11A, CCL21, IL15RA, CSF3R, IFNGR1, IL1A, LTBR, IL6R, CCL18, TNFSF10, CCL13, TNFSF11, CCL14, TNFSF13B, CXCL14, CXCL16, CX3CR1, IL12B, XCL2, IL3RA*	1.04e-17	0.189
Cell adhesion molecules (CAMs)	7.2	*CDH1, ITGB2, ITGB1, PDCD1LG2, CDH5, VCAM1, NCAM1, SIGLEC1, CD86, ITGA6, CD34, ICOS, PECAM1, CD4, SELPLG, CD28*	7.25e-8	0.9
T-cell costimulation and signaling activation	11.6	*CD86, CD3G, CD3D, TNFSF13B, CD3E, CCL21, ICOS, CD247, CD4, DPP4, PDCD1LG2, CD28, ITK*	4.34e-5	**0.035**
Natural killer cell mediated cytotoxicity	4.2	*CD244, SH2D1A, TNFSF10, CD247, FCER1G, ITGB2, KLRD1, IFNGR1*	0.01	0.205

adj.P. Val: adjusted p-value; COX reg. P. Val: COX regression p-value

Supplemental Table S8. DAVID gene ontology functional annotations of the 66 NanoString-based downregulated genes in SOX11+ vs. SOX11- nodal MCLs and RLN primary cases, without significant expression differences between the unpurified and purified MCL nodal samples, and their association with OS of 122 SOX11+ MCL patients (GSE93291).

Functional annotation cluster	Enrichment score	Genes	adj. P. Val	COX reg. P. Val
Antigen processing and presentation	2.73	*HLA-E, HLA-DPA1, HLA-DPB1*	0.031	**0.0195**
Cytokine-cytokine receptor interaction	2.72	*CCL16, CCL23, CCR2, CCR4, CCR9, FLT3LG, IL18RAP, IL2, IL2RG, IL23R, TNFSF18, TNFRSF10C, TNFRSF8*	1.5e-5	0.674

adj.P.Val: adjusted p-value; COX reg. P. Val: COX regression p-value

Supplemental Table S9. Differential expression of the 24 genes, significantly upregulated in SOX11+ compared to SOX11- nodal MCLs and RLNs, in CD19+ purified lymph nodes (CD19+LN; n=4) compared to unpurified nodal samples of pretreated MCL cases (unpurified LN; n=34) and CD19+ purified peripheral blood samples (CD19+PB; n=15) (GSE70910).

	Unpurified LN vs CD19+LN		CD19+PB vs CD19+LN	
	log2(FC)	adj.P.val	log2(FC)	adj.P.val
BCL2	1,006	0,003	0,122	0,614
ILF3	0,990	0,066	1,054	0,066
CD70	**0,906**	**0,021**	**0,893**	**0,023**
SYT17	0,759	0,131	-0,772	0,141
CEACAM1	0,755	0,026	0,486	0,131
IL17RB	0,615	0,383	1,843	0,033
TNFRSF13C	0,588	0,008	-0,184	0,248
MSR1	0,533	0,585	0,846	0,383
CD19	0,518	0,009	0,460	0,020
PRKCE	0,469	0,083	-0,723	0,021
IRF5	0,465	0,460	-0,311	0,645
PAX5	0,447	0,010	-0,253	0,088
TFEB	0,408	0,051	-0,221	0,248
CD24	0,340	0,131	0,680	0,020
MYD88	0,182	0,094	0,135	0,222
SH2B2	0,139	0,645	-0,112	0,709
STAT6	0,100	0,768	-0,042	0,913
TLR9	-0,019	0,922	0,352	0,185
CXCR5	-0,115	0,709	0,395	0,248
ENTPD1	-0,118	0,759	0,531	0,224
CD79A	-0,630	0,266	-0,473	0,442
CD79B	-0,961	0,023	-0,135	0,709
CD37	-1,168	0,102	-1,274	0,094
TNFRSF9	-3,604	0,000	0,835	0,094

FC: Fold Change; adj.P.Val: adjusted p-value

Supplemental Table S10. Univariate and multivariate linear regression models of CD70 protein expression estimated with our series of MCL primary cases. The intercept terms of the models are not shown.

	Univariate			Multivariate		
	Coef.	**IC95%**	**P-value**	**Coef.**	**IC95%**	**P-value**
SOX11 positivity	21.54	[7.47,35.61]	0.003	25.95	[15.07,36.82]	<0.001
Blastoid/Pleomorphic variant	32.00	[19.28,44.72]	<0.001	27.91	[14.22,41.61]	<0.001
Ki67 index	0.41	[0.21,0.61]	<0.001	0.18	[-0.02,0.39]	0.076

Coef.= Coefficient; n=64; Multivariate model adjusted R-squared = 0.48

Supplemental Table S11. Pairwise multivariate Cox regression models used to evaluate the independent prognostic value of CD70 protein expression in presence of other risk factors (Ki67 index, *TP53* alterations or the blastoid/pleomorphic cytological variant), estimated with our series of SOX11+ nodal MCL primary cases. Hazard ratios (HR) for Ki67 index and CD70 protein expression correspond to 10 units increments.

	HR	IC95%	P-value
CD70 protein expression	1.36	[1.05,1.78]	0.022
***TP53* alterations**	2.08	[0.48,9.09]	0.330

n=33, events=14; Global test p-value = 0.01
TP53 alterations (mutations, deletions and/or protein overexpression)

	HR	IC95%	P-value
CD70 protein expression	1.55	[1.17,2.05]	0.002
Blastoid/Pleomorfic Variant	0.23	[0.05,1.13]	0.071

n=40, events=14; Global test p-value = 0.01

	HR	IC95%	P-value
CD70 protein expression	1.22	[0.88,1.69]	0.242
Ki67 Index	1.07	[0.80,1.44]	0.653

n=40, events=14; Global test p-value = 0.06

Supplemental Table S12. Univariate and multivariate Cox regression models estimated with the 122 nodal MCL samples cohort (GSE93291). One outlier sample was removed in the models that included the T cell costimulation and receptor signaling score. Hazard ratios (HR) for FOXP3/CD3 mRNA ratio correspond to 0.1 units increments.

	Univariate			Multivariate		
	HR	**IC95%**	**P-value**	**HR**	**IC95%**	**P-value**
CD70 mRNA expression	1.36	[1.06,1.76]	0.017	1.02	[0.78,1.34]	0.877
FOXP3/CD3 mRNA ratio	1.33	[1.04,2.06]	0.049	1.42	[1.04,1.94]	0.028
T cell costimulation and signaling activation	0.67	[0.46,0.97]	0.036	0.82	[0.56,1.21]	0.321
MKI67 mRNA expression	2.48	[1.90,3.25]	<0.001	2.51	[1.88,3.35]	<0.001

n=122, events=80; Multivariate model global test p-value<0.001.

SUPPLEMENTAL FIGURES
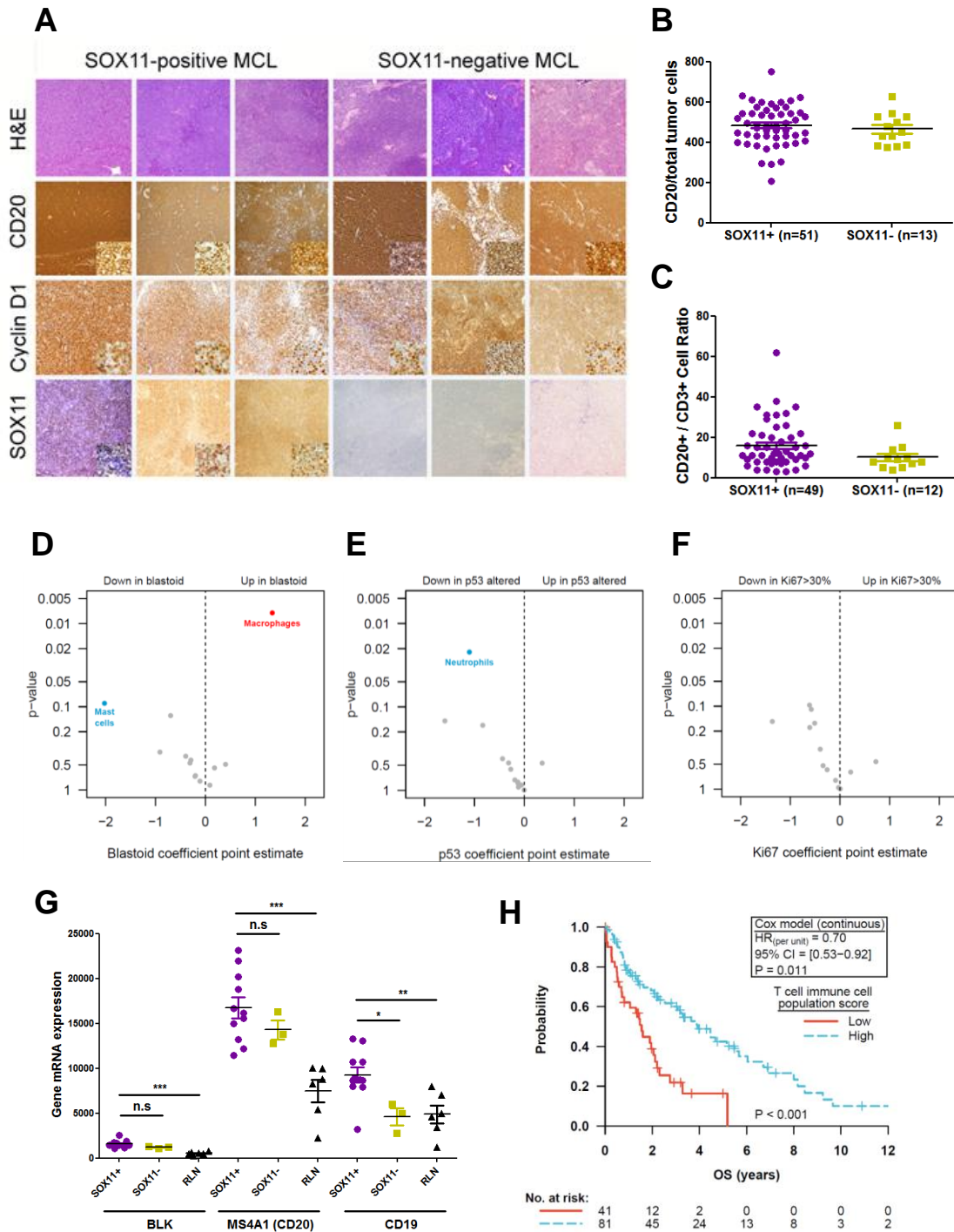
Supplemental Figure S1. Low T cell population is associated with significant shorter OS of patients with MCL. (A) SOX11+ and SOX11- nodal MCL primary samples have the same tumor cell content. Representative histological sections from SOX11+ and SOX11-nodal MCL primary samples stained with Hematoxylin and

Eosin (H&E) and specific antibodies anti-human CD20, Cyclin D1 and SOX11(x40), Inset magnification (x400). **(B)** IHC quantifications of CD20+ tumor cells and **(C)** CD20+/CD3+ cell ratio in SOX11+ and SOX11- nodal MCLs. **(D-F)** Volcano plots representing the effect of the risk factors: Blastoid/pleomorphic variant **(D)**, *TP53* alterations (mutations, deletions and/or protein overexpression) **(E)**, and high Ki67 (Ki67>30%) **(F)**, on the immune cell population scores, estimated with linear regression models that also included the subgroup of the samples (SOX11+, SOX11- and RLN). The effect of each risk factor was estimated without including the other risk factors in the linear models. Analyses performed with the immune cell population scores marked in red or blue within a risk factor were adjusted by that factor, as it was considered a potential confounding variable. **(G)** mRNA expression of BLK, MS4A1 (CD20) and CD19, used by the nSolver to defined B-cell content score, based on NanoString analysis in SOX11+, SOX11- nodal MCL and RLN primary samples.*p<0.05, **p<0.01, ***p<0.001. **(H)** Kaplan-Meier curve and Cox regression showing the association of the T cell population score with OS, using 122 SOX11+nodal MCL cases previously published (GSE93291). The score was calculated as the average expression of the specific T cell immune subtype markers (CD3D, CD3G, CD3E, SH2D1A) (Figure 1). High values were defined by Maxstat (cutoff point=8.8). The log-rank test p-value, the hazard ratio (HR) with 95% confidence interval (CI), and the Cox regression p-value are shown.
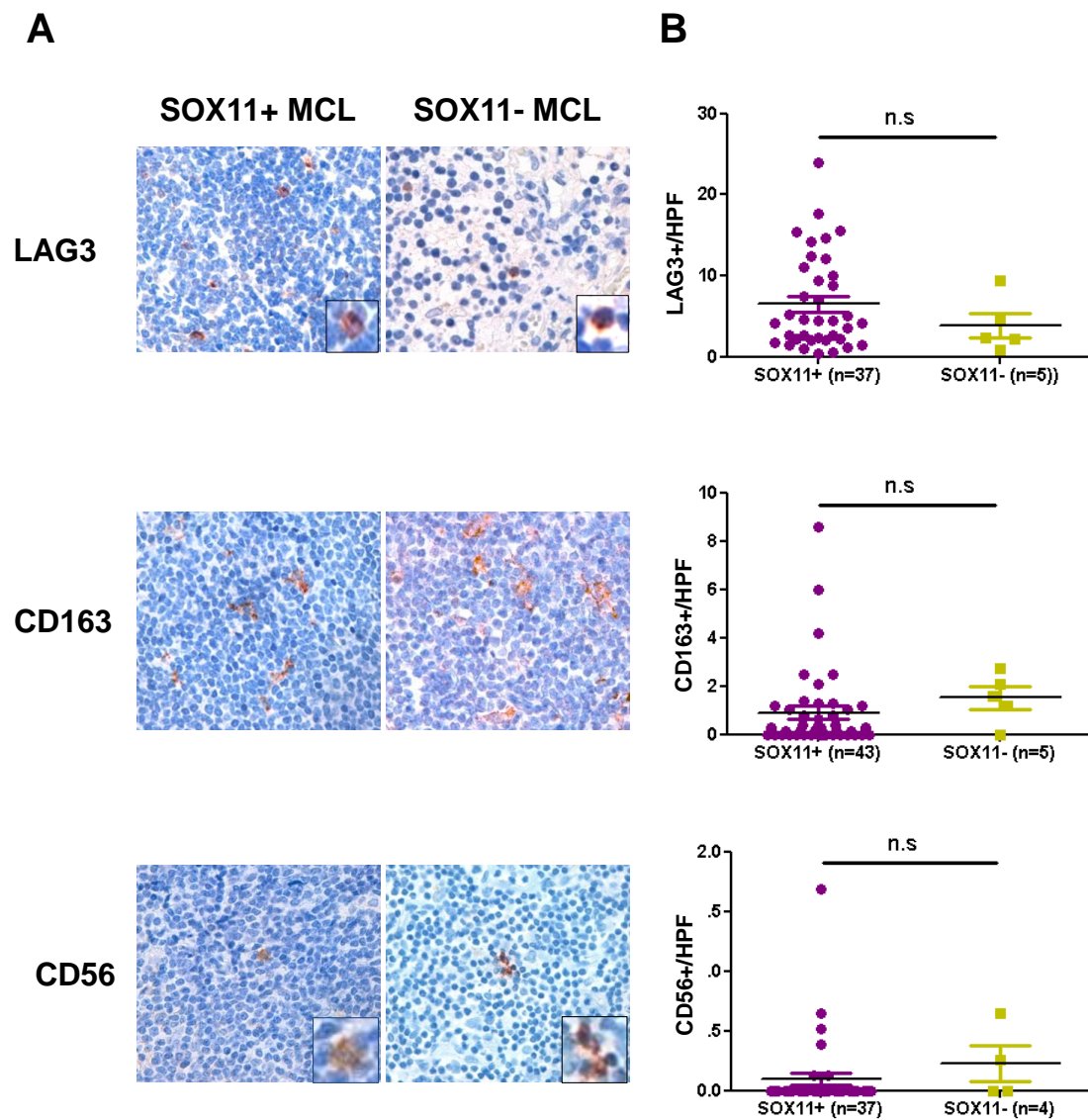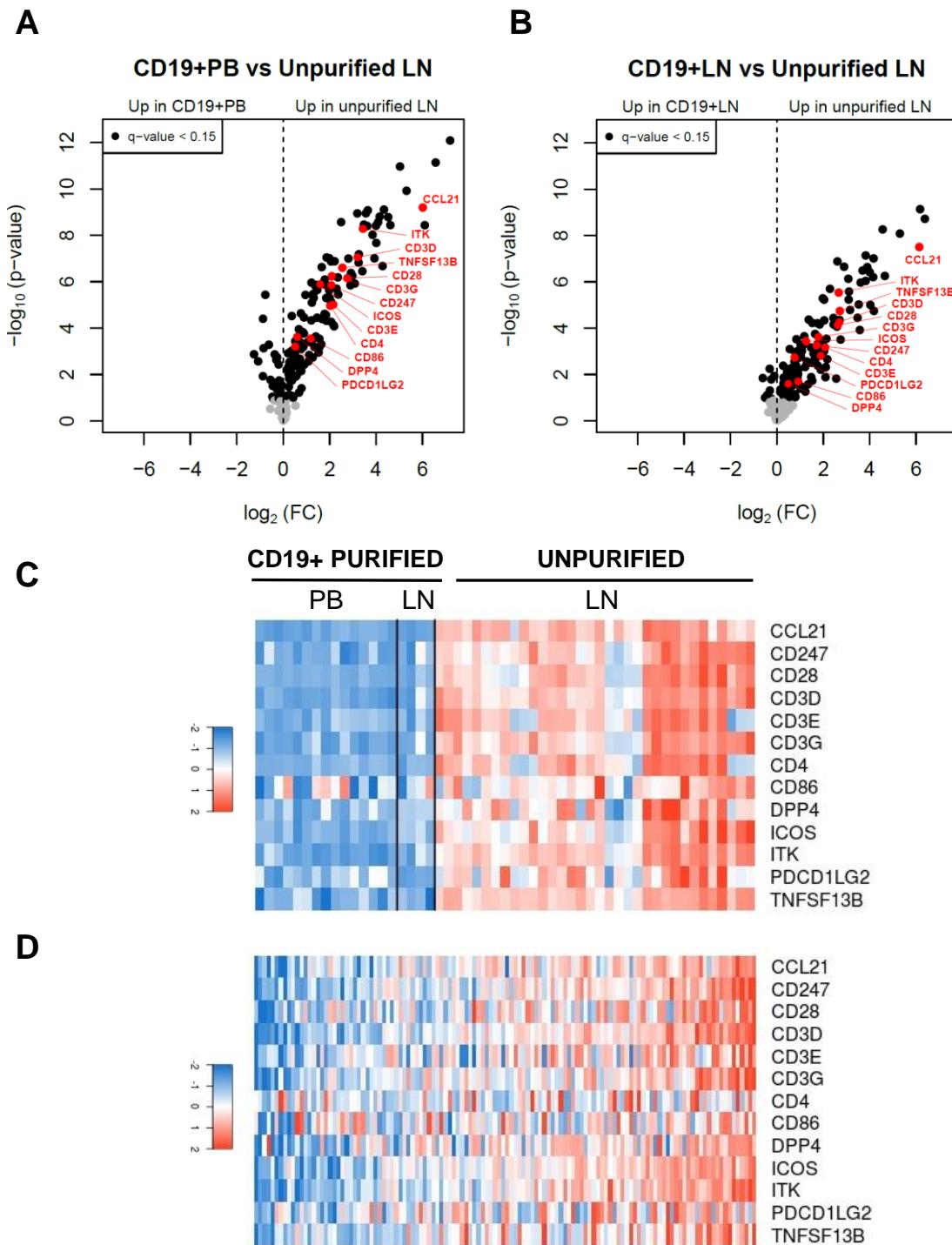
Supplemental Figure 2. CD56+ NK cells, CD163+ TAMs and LAG3+ exhausted T cells in SOX11+ and SOX11- nodal MCL primary cases. (**A**) Representative histological sections from SOX11+ and SOX11- nodal MCLs stained with specific anti-human LAG3, CD163 and CD56 antibodies. Pictures contain insets with magnification. (**B**) IHC quantifications of LAG3, CD163 and CD56+ stained intratumoral cells in SOX11+ and SOX11- nodal MCLs. The significance of difference was determined by independent samples Student t test: n.s.=statistically not significant. HPF: Number of positive cells per high power field (x400)

A SOX11− vs SOX11+

B RLN vs SOX11+

C RLN vs SOX11−

D Blastoid effect to gene expression

E p53 effect to gene expression

F Ki67 effect to gene expression
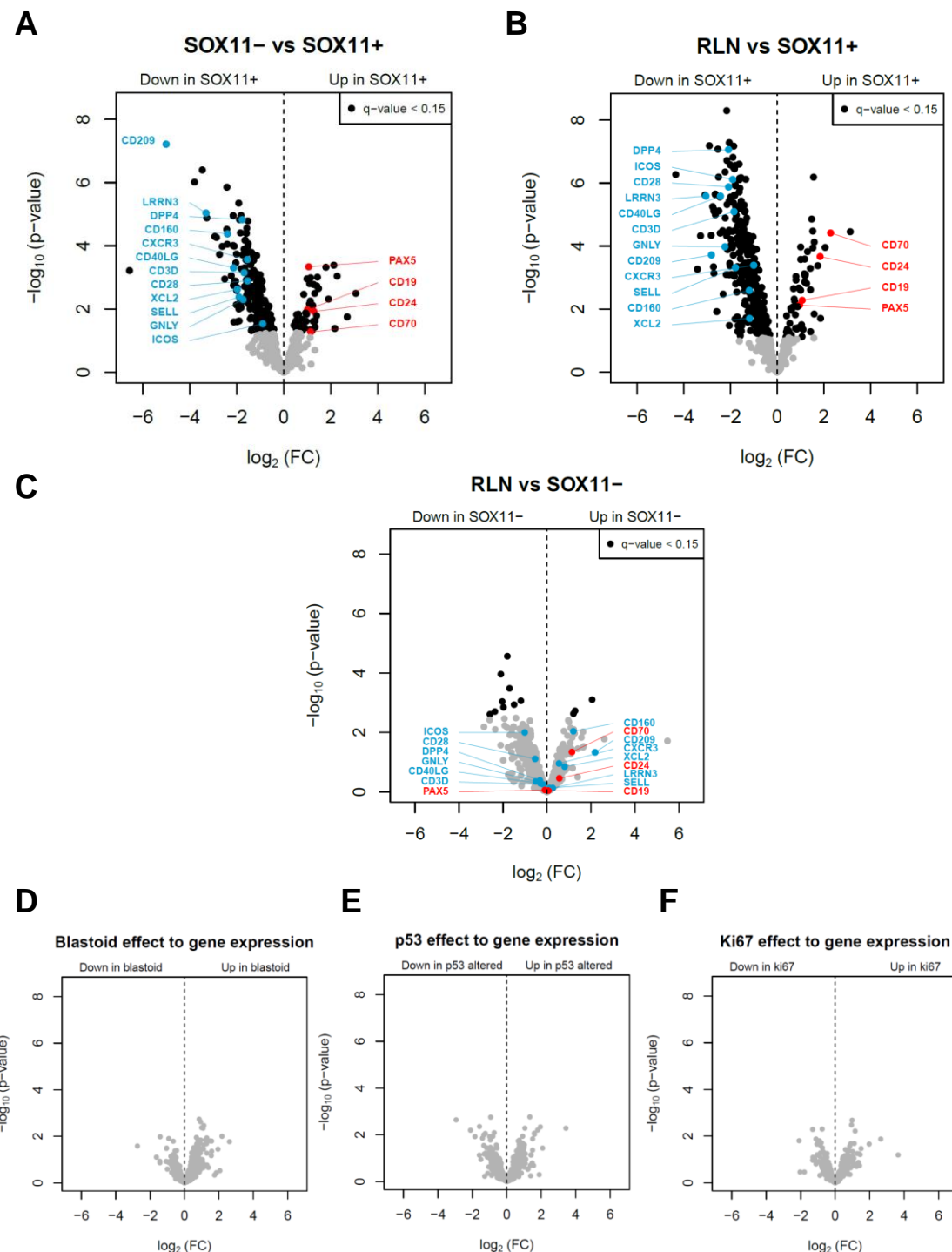
Supplemental Figure S3. NanoString-based GEP reveals that most of the immune-related genes are downregulated in SOX11+ compared to SOX11- MCL and RLN samples. Volcano plots representing the differential gene expression of the immune-related genes in SOX11+ nodal MCL primary samples (SOX11+; n=11) compared to (**A**) SOX11- cases (SOX11-; n=3) and (**B**) RLN

samples (RLN; n=6). **(C)** Volcano plot representing the differential gene expression of the immune-related genes in SOX11- nodal MCL primary samples (SOX11-; n=3) compared to RLN samples (RLN; n=6). Volcano plots display each gene p-value and fold change (FC) in -log10 and log2, respectively. Genes with adjusted p-value (q-value) ≤0.15 are marked with black spots. Representative genes upregulated in SOX11+ (colored in red) or downregulated in SOX11+ (colored in blue) are written inside the volcano graphs. **(D-F)** Volcano plots representing the effect of the risk factors blastoid/pleopmorphic variant **(D)**, *TP53* alterations (mutations, deletions and/or protein overexpression) **(E)** and high Ki67 **(F)** on the NanoString expression of the immune-related genes, estimated with linear regression models that also included the subgroup of the samples (SOX11+, SOX11- and RLN). The effect of each risk factor was estimated without including the other risk factors in the linear models. Volcano plots display each gene p-value and fold change (FC) in -log10 and log2, respectively. The expression of any specific gene was clearly affected by the risk factors.

Supplemental Figure S4. Most of the downregulated immune genes in SOX11+ compared to SOX11- MCLs and RLN are expressed by the non-malignant cells present in the lymph node microenvironment. Volcano plots of 190 genes, significantly downregulated in SOX11+ compared to SOX11- nodal MCLs and RLNs, representing the differential gene expression in unpurified nodal samples

(unpurified LN; n=34) compared to **(A)** CD19+ purified lymph nodes (CD19+LN; n=4) and **(B)** CD19+ purified peripheral blood samples (CD19+PB; n=15) of pretreated MCL cases (GSE70910). Volcano plots display each gene p-value and fold change in -log10 and log2, respectively. Genes with adjusted p-value (q-value)≤0.15 are marked with black spots. The 13 genes grouped in the T-cell costimulation and signaling activation GO pathway are colored in red. Heatmaps showing the expression of the 13 genes grouped in the T-cell costimulation and signaling activation GO pathway, in the previously published datasets **(C)** GSE70910 (34 unpurified lymph nodes, 4 CD19+ purified lymph nodes, and 15 peripheral blood samples) and **(D)** GSE93291 (122 SOX11-positive nodal MCL cases). Red in the heatmap represents high expression and blue indicates low expression.

A

Unpurified LN vs CD19+LN

Up in unpurified LN   Up in CD19+LN

● q-value < 0.15

TNFRSF9

BCL2
TNFRSF13C
CD19
PAX5
CD70
CEACAM1
TFEB
ILF3
PRKCE
MYD88
SYT17
CD24

CD79B
CD37

$-\log_{10}$ (p-value)

$\log_2$ (FC)

B

CD19+PB vs CD19+LN

Up in CD19+PB   Up in CD19+LN

● q-value < 0.15

PRKCE
PAX5
CD37
SYT17

CD19
CD24
CD70
IL17RB
ILF3
TNFRSF9
CEACAM1

$-\log_{10}$ (p-value)

$\log_2$ (FC)

C

CD19+ PURIFIED   UNPURIFIED

PB   LN   LN

TNFRSF9
CD19
CD70 ◄
PAX5
BCL2
PRKCE
TNFRSF13C
CD24
CEACAM1
ILF3
CD37
IL17RB
TFEB
CD79B
SYT17
MYD88
CD79A
ENTPD1
TLR9
CXCR5
MSR1
IRF5
SH2B2
STAT6

-2 -1 0 1 2

D

IHC

Pearson r= 0.643
P value = ** 0.013
N = 14

Nanostring

Supplemental Figure S5. CD70 has a differential tissue-dependent expression, with a significant higher mRNA levels in CD19+ MCL cells purified from lymph node than from peripheral blood and unpurified lymph node primary MCL samples. Volcano plots of 24 genes, significantly upregulated in SOX11+ compared to SOX11- nodal MCLs and RLNs, representing the differential gene expression in CD19+ purified nodal samples (CD19+LN; n=4) compared to **(A)** unpurified lymph

nodes (unpurified LN; n=34) and **(B)** CD19+ purified peripheral blood samples (CD19+PB; n=15) of pretreated MCL cases (GSE70910).Volcano plots display each gene p-value and fold change in -log10 and log2, respectively. Genes with adjusted p-value (q-value)≤0.15 are marked with black spots and written inside the volcano graphs. Representative genes upregulated in CD19+ LN (colored in red) or downregulated in CD19+ LN (colored in blue) are written inside the volcano graphs. **(C)** Heatmap showing the expression of the common 24 genes, statistically significant upregulated in SOX11+ compared to SOX11- MCLs and RLNs, in the previously published data of 34 unpurified nodal MCL (UNPURIFIED LN), 4 CD19+ purified lymph nodes (LN) and 15 CD19+ purified cells from the peripheral blood (PB) samples (GSE70910). Red in the heatmap represents high expression and blue indicates low expression. CD70 mRNA overexpression in CD19+ purified LN compared to the other compartments is marked by a red arrow. **(D)** Positive correlation between CD70 mRNA expression and CD70+ cells, analyzed by NanoStringand IHC, respectively, in 11 SOX11+ and 3 SOX11- nodal MCL cases. Graphs show Pearson correlation coefficient (r), p value and number of cases analyzed (N).
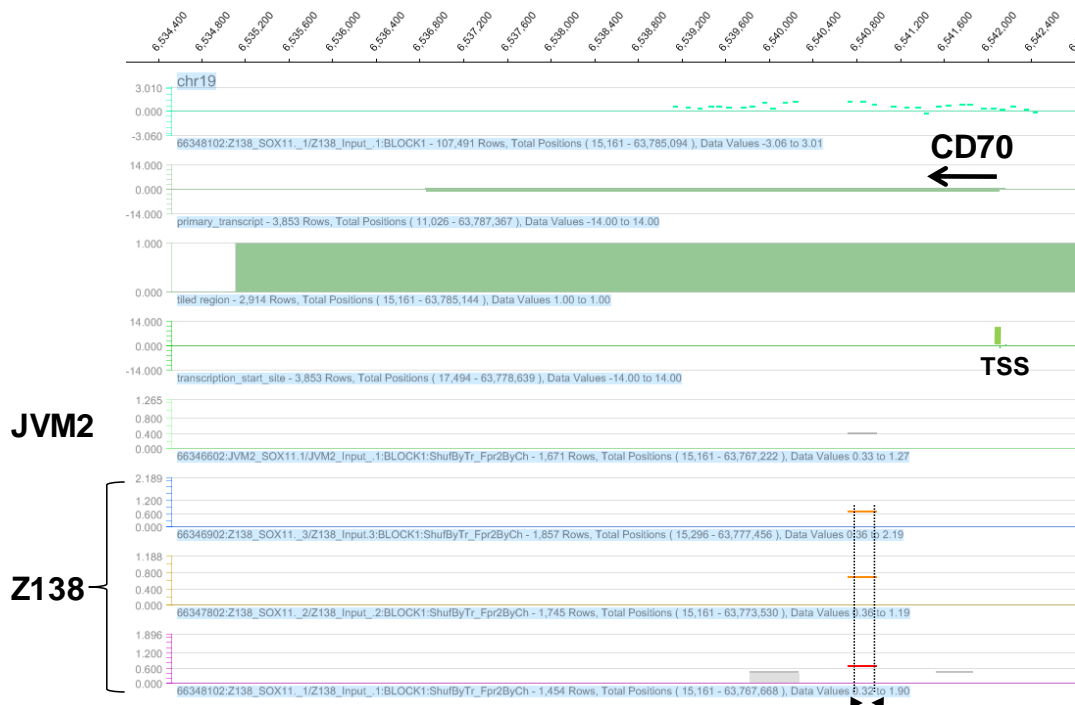
Supplemental Figure S6. *In vitro* **SOX11-specific binding to** *CD70* **regulatory region.** SignalMap representation of SOX11-specific binding to *CD70* regulatory region identified by ChIP-chip in three replicates of the SOX11-expressing MCL cell line, Z138.[1] These peaks were very weak in the SOX11-negative MCL cell line, JVM2. Red lines at the bottom depict high confidence peaks identified by Nimblescan peak finding algorithm. Orange, yellow and grey lines represent from poor, very poor to negative peaks also identified by Nimblescan peak finding algorithm. Position of gene transcripts and the promoter regions analyzed in the NimbleGen Human ChIP-chip 2.1 M Deluxe promoter array (spanning from 5kb upstream to 1kb downstream of transcription start site (TSS)) are represented in the middle panel in green, and correspond to the human genome assembly browser NCBI36/hg18. The black arrows below the red peaks indicate the primers sequences used to validate the SOX11-binding region by ChIP-qPCR.
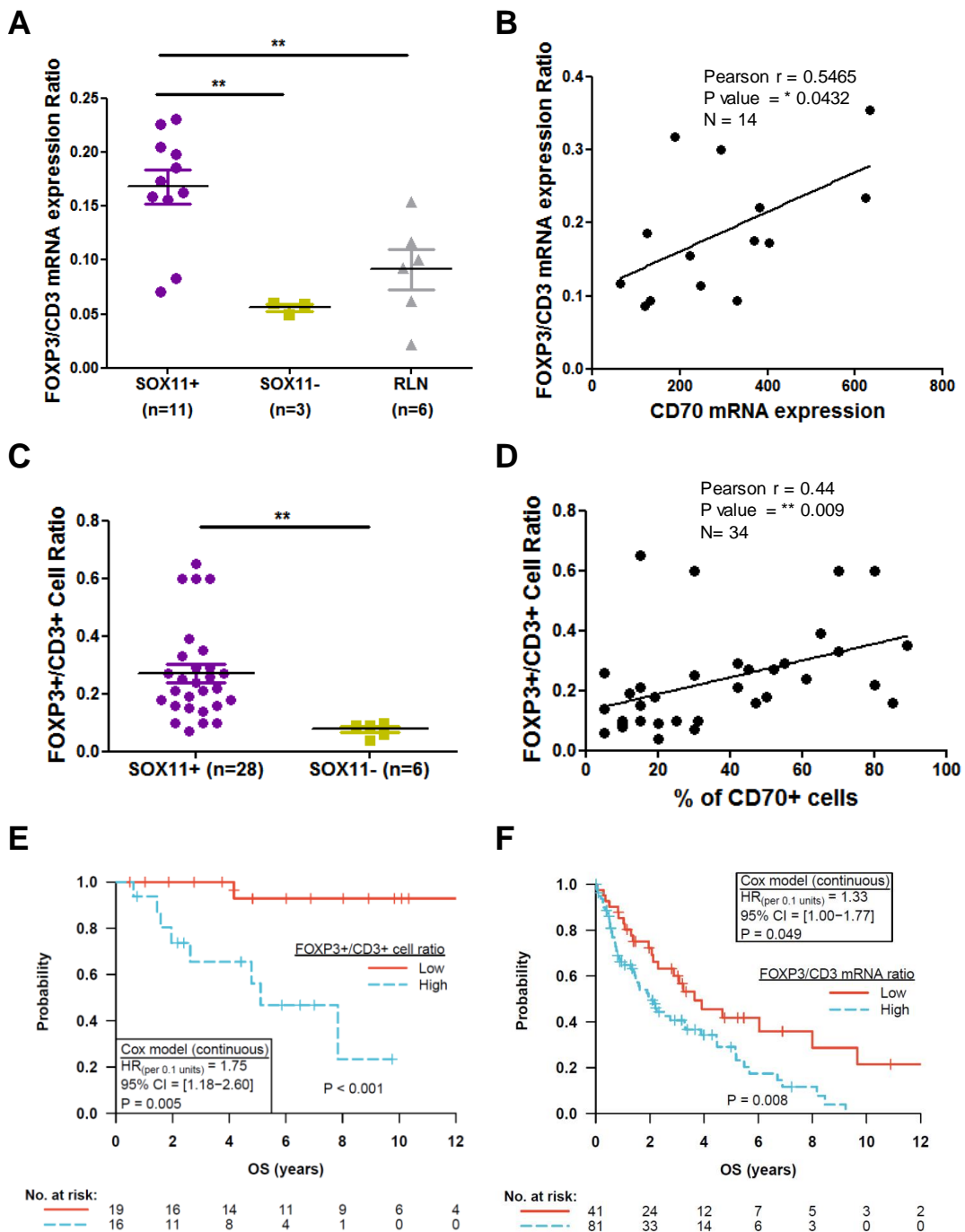
Supplemental Figure S7. FOXP3/CD3 mRNA and protein cell ratios are higher in SOX11+ compare to SOX11- nodal MCL and RLN primary samples and positively correlate with CD70 expression in MCL cells. (A) FOXP3/CD3 mRNA ratio data based on NanoString data in 11 SOX11+ and 3 SOX11- nodal MCLs and 6 RLN primary samples. **(B)** Positive correlation between NanoString-based CD70

42

mRNA expression and FOXP3/CD3 mRNA ratio. **(C)** IHC quantification of FOXP3+/CD4+ T-cell ratio in our series of SOX11+ (n=28) and SOX11- (n=6) primary nodal MCLs samples. **p<0.01. **(D)** Positive correlation between CD70+ cells and FOXP3+/CD3+ T-cell ratio, quantified by IHC in our series of nodal MCL. Graphs show Pearson correlation coefficient (r), p value and number of cases analyzed (N). **(E)** Kaplan-Meier curve and cox regression showing the association of FOXP3+/CD3+ cell ratio, quantified by IHC in our series of nodal MCL, with OS. High values were defined by Maxstat (cutoff point=0.21). **(F)** Kaplan-Meier curve and cox regression showing the association of FOXP3/CD3 mRNA ratio with OS, using previously published GEP and clinical data from 122 nodal SOX11+ MCL primary cases (GSE93291). High values were defined by Maxstat (cutoff point=0.514). The log-rank test p-value, the hazard ratio (HR) with 95% confidence interval (CI), and the cox regression p-value are shown.

A

B

C

D
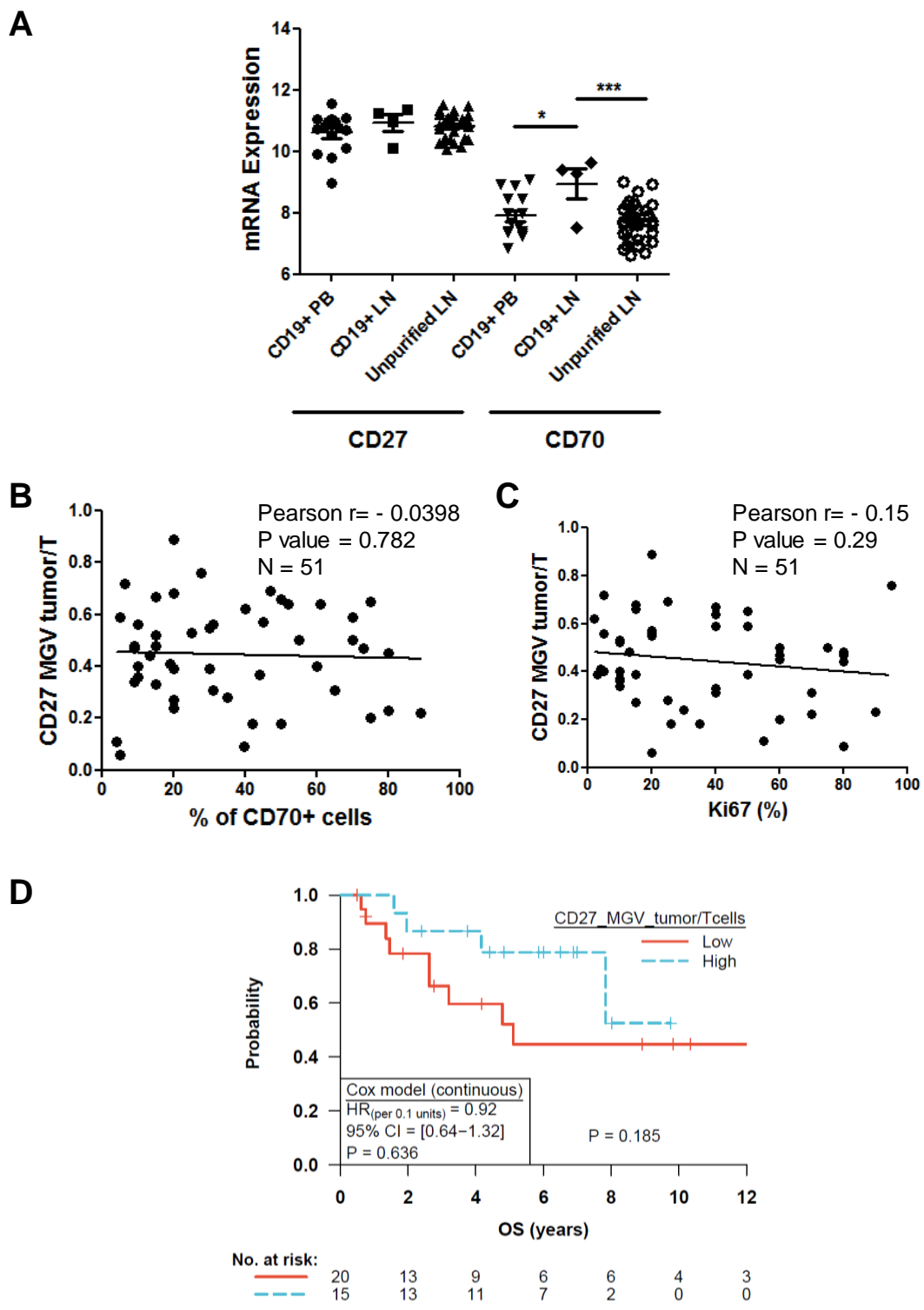
Supplemental Figure S8. CD27 expression in nodal MCL. (A) CD27 and CD70

mRNA expression levels in unpurified lymph node MCL samples (Unpurified LN;

n=34), CD19+ purified cells from lymph node samples (CD19+ LN; n=4) and

peripheral blood samples (CD19+ PB; n=15) (GSE70910). *Q-value<0.15, ***Q-

value<0.05. **(B-C)** Lack of correlation between CD27 mean gray value (MGV) tumor/T cells and CD70+ cells **(B)** or Ki67 **(C)**, quantified by IHC in our series of nodal MCL. Graphs show Pearson correlation coefficient (r), p value and number of cases analyzed (N). **(D)** Kaplan-Meier curve and cox regression showing the association of CD27 MGV tumor/T cells by IHC with OS, using our series of SOX11+ nodal MCL primary samples. High values were defined by Maxstat (cutoff point=0.47). The log-rank test p-value, the hazard ratio (HR) with 95% confidence interval (CI), and the Cox regression p-value are shown.

REFERENCES

1. Vegliante MC, Palomero J, Perez-Galan P, et al. SOX11 regulates PAX5 expression and blocks terminal B-cell differentiation in aggressive mantle cell lymphoma. *Blood*. 2013;121(12):2175-2185.

2. Balsas P, Palomero J, Eguileor A, et al. SOX11 promotes tumor protective microenvironment interactions through CXCR4 and FAK regulation in mantle cell lymphoma. *Blood*. 2017;130(4):501-513.

3. Veloza L, Teixido C, Castrejon N, et al. Clinicopathological Evaluation of PD1/PD-L1 Axis in Post-Transplant Lymphoproliferative Disorders: Association with EBV, PD-L1 Copy Number Alterations and Outcome. *Histopathology*. 2019; 75(6):799-812.

4. Soldini D, Valera A, Sole C, et al. Assessment of SOX11 expression in routine lymphoma tissue sections: characterization of new monoclonal antibodies for diagnosis of mantle cell lymphoma. *Am J Surg Pathol*. 2014;38(1):86-93.

5. Crowe AR, Yue W. Semi-quantitative Determination of Protein Expression using Immunohistochemistry Staining and Analysis: An Integrated Protocol. *Bio Protoc*. 2019;9(24):e3465.

6. Bankhead P, Loughrey MB, Fernández JA, et al. QuPath: Open source software for digital pathology image analysis. *Sci Rep*. 2017;7(1):16878.

7. Saba NS, Liu D, Herman SE, et al. Pathogenic role of B-cell receptor signaling and canonical NF-kappaB activation in mantle cell lymphoma. *Blood*. 2016;128(1):82-92.

8. Navarro A, Clot G, Martínez-Trillos A, Pinyol M, Improved classification of leukemic B-cell lymphoproliferative disorders using a transcriptional and genetic classifier. *Haematologica*. 2017;102(9):e360-e363.

9. Clot G, Jare P, Giné E, et al. A gene signature that distinguishes conventional and leukemic nonnodal mantle cell lymphoma helps predict outcome.*Blood.* 2018;132(4):413-422.

10. Scott DW, Abrisqueta P, Wright GW, et al. New Molecular Assay for the Proliferation Signature in Mantle Cell Lymphoma Applicable to Formalin-Fixed Paraffin-Embedded Biopsies. *J Clin Oncol*. 2017;35(15):1668-1677.